Measurement of Cytosolic Free Magnesium Ion Concentration by ^{19}F NMR

Louis A. Levy, Elizabeth Murphy, B. Raju, and Robert E. London*

Laboratory of Molecular Biophysics, National Institute of Environmental Health Sciences, P.O. Box 12233, Research Triangle Park, North Carolina 27709

Received September 2, 1987; Revised Manuscript Received January 21, 1988

ABSTRACT: Fluorinated derivatives of the chelator *o*-aminophenol-*N*,*N*,*O*-triacetic acid (APTRA) have been developed, synthesized, and analyzed for use as ^{19}F NMR indicators of free cytosolic magnesium concentration. Magnesium dissociation constants for the 4-fluoro, 5-fluoro, and 4-methyl-5-fluoro species were determined to be 3.1, 0.9, and 0.6 mM, respectively, on the basis of UV absorption measurements at 37 °C in 115 mM KCl and 20 mM NaCl, pH 7.1, buffered with 4-(2-hydroxyethyl)-1-piperazineethanesulfonic acid–tris(hydroxymethyl)aminomethane. The corresponding pK values, which reflect protonation of the nitrogen atom, were determined by ^{19}F NMR to be 4.15, 5.45, and 5.55, respectively, so that the chelators are insensitive to pH variations near the normal physiological range. The dissociation constants of these chelators for calcium ions are lower than those for magnesium but roughly 2–3 orders of magnitude above typical basal cytosolic free calcium levels, so that calcium ions will not interfere with the determinations of magnesium levels. ^{19}F NMR studies carried out at 339.7 MHz indicate that magnesium ions are in slow exchange with the 5-fluoro and 4-methyl-5-fluoro APTRA derivatives and in fast exchange with the 4-fluoro APTRA derivative. In contrast, calcium ions were found to be in intermediate to fast exchange with all chelators. The apparent anomaly of higher thermodynamic stability of the APTRA complexes for calcium relative to magnesium but lower kinetic stability (higher k_{-1} values) for the calcium complexes reflects the very different association rates for the two ions. Thus, the magnesium association rates are 3 orders of magnitude slower than those for calcium ions. As in the case of the structurally analogous 1,2-bis(2-aminophenoxy)ethane-*N*,*N*,*N*′,*N*′-tetraacetic acid analogues that have been used as intracellular calcium indicators, the acetoxymethylated derivatives of these chelators load readily into a variety of cell types. ^{19}F NMR studies of 4-methyl-5-fluoro-APTRA-loaded human erythrocytes indicate a basal free magnesium level of 0.25 mM.

The importance of magnesium ions as a cofactor for cellular enzymes and transporters has long been recognized (Wacker, 1969; Murphy et al., 1969; Skou, 1975). Additional interest has been focused on the ability of magnesium to compete with calcium ions for binding sites and thereby modulate the response of cellular components to changes in cytosolic calcium levels (Ostwald & MacLennan, 1974; Iseri & French, 1984), as has been demonstrated recently for the release of calcium ions by sarcoplasmic reticulum (Meissner & Henderson, 1987).

Corkey et al. (1986) have shown that magnesium ions are well-buffered intracellularly, providing a stable level for many magnesium-dependent cellular enzymes and transporters. However, this level of buffering makes it an unlikely candidate to function as an acute intracellular messenger. In keeping with this view, Flatman (1984) and Grubbs and Maguire (1987) have suggested that slow, small changes could be important in fine control and coordination of cell activity. This view is consistent with the association between hypomagnesemia and disease states (Whang, 1987; Altura & Altura 1981; Corkey et al., 1986; Fuji et al., 1982).

In addition, there are several reports suggesting an acute role for cytosolic magnesium ions in metabolic regulation. Stern et al., (1987) have proposed that magnesium may function as an intracellular signal in retinal rods; Bond et al. (1987) showed an acute increase in liver mitochondrial total magnesium after injection of a rat with vasopressin and glucagon. In addition, glucose (Henquin, 1983) and β-agonist (Macquire & Eros, 1980) are reported to alter magnesium fluxes across the plasma membrane.

Evaluation of the role of magnesium as an acute or chronic regulator of cell function has been limited by the availability of direct methods for measuring cytosolic, ionized magnesium levels ("free magnesium") in small mammalian cells. Presently available methods for measuring magnesium include indirect calculations based on equilibrium reactions (Veloso et al., 1973), NMR observations of molecules such as ATP (Gupta & Yushok, 1980; Garfinkel & Garfinkel, 1983) and citrate (Cohen, 1983) that chelate magnesium ions, ion-selective microelectrodes (Lopez et al., 1984; Fry, 1986), and null point measurements using metallochromic dyes that are either microinjected into cells (Brinley & Scarpa, 1975) or placed into the extracellular space with subsequent lysis of the cells (Rink et al., 1982; Corkey et al., 1986). Many of these approaches involve destruction of the cells during the measurement; only the ion-selective electrodes, the microinjection of metallochromic dyes, and the in vivo NMR measurements allow essentially continuous measurements on the same cells. The metallochromic dyes can only be used directly in large cells suitable for microinjection. Ion-selective microelectrode measurements are subject to interference from sodium (Fry, 1986), although this technology has continued to improve. In the case of in vivo ^{31}P NMR studies of cytosolic ATP (Phillips et al., 1986), the relatively low value for K_D^{Mg} of 0.1 mM limits the accuracy of the determination since in most cells the ATP will be nearly saturated with magnesium. The determination of Mg^{2+} based on the ^{13}C-shifted resonances of citrate is limited to studies involving ^{13}C-labeled metabolites and is subject to the inherently low sensitivity of ^{13}C observations and to uncertainties resulting from the possible compartmentation of the citrate. Additionally, questions about the stoichiometry of the magnesium citrate complex remain to be addressed. In vivo ^{1}H NMR studies of citrate might eventually prove useful if the technological difficulties with in vivo ^{1}H NMR studies arising primarily from the need to suppress the intense water

resonance can be solved. Preliminary data on the use of fluorocitrate as an indicator for cell magnesium have also recently been reported (Morris et al., 1987).

The strategy of introducing fluorescent chelators into cells in order to measure cytosolic free calcium ion levels has been pioneered by Tsien (1980), and this approach has been subsequently extended by Smith et al. (1983) with the introduction of fluorinated chelators that can be studied in vivo by using ^{19}F nuclear magnetic resonance. In principle, the extension of such strategies to the study of cytosolic magnesium ion levels is straightforward and requires the development of chelators with magnesium K_D values close to the physiological range of 1 mM and with K_D values for other cellular ions well outside the physiological levels. In the present study, we describe the preparation and use of fluorinated derivatives of *o*-aminophenol-*N*,*N*,*O*-triacetic acid (APTRA)[1] that satisify most of the above criteria and have been used to carry out determinations of cytosolic magnesium levels in erythrocytes.

Design Considerations. The use of intracellular chelators for the determination of cytosolic calcium levels requires that such chelators exhibit high selectivity for calcium relative to magnesium, since the ratio of the concentrations of the free ion pools is in the range 1:10000. The fluorescent and fluorinated NMR sensitive chelators that have been developed for such determinations are derivatives of EGTA which possess the necessary selectivity. This selectivity is believed to arise from the size of the ion cavity formed by the chelator being appropriate to ionic radius of Ca^{2+} vs Mg^{2+} (Tsien, 1980). Consequently, a possible beginning point for the development of an intracellular magnesium chelator involves derivatization of EDTA, $(^{-}O_2CCH_2)_2NCH_2CH_2N(CH_2COO^{-})_2$, which is characterized by a considerably smaller cavity and by a considerably lower ability to discriminate between calcium and magnesium ions. Analogous to the strategies developed by Tsien (1980) and extended by Smith et al. (1983), the EDTA structure can be made less sensitive to changes in pH (i.e., the amino p*K* values lowered) and the needed reporter group, in this case fluorine, introduced via the replacement of the central ethylene moiety with a fluorinated benzene. However, the synthesis of fluorinated *o*-phenylenediamine-*N*,*N*,*N*′,*N*′-tetraacetic acid is extremely difficult, presumably due to steric effects. Thus, *p*-phenylenediaminetetraacetic acid is commercially available, but the ortho derivative is not.

We therefore substituted one of the amino groups with an oxygen substituent that could be carboxymethylated via an ether linkage. The resulting derivative, fluorinated in the aromatic portion, yielded chelators with the desired NMR sensitivities. As a consequence of the structural analogy between the fluorinated *o*-aminophenol-*N*,*N*,*O*-triacetic acid (APTRA) and BAPTA, the effects of chelation on the fluorine chemical shifts and the effects of placement of the fluorine substituent on dissociation constants are largely predictable (Smith et al., 1983; Levy et al., 1987). In this study the three fluorinated derivatives 4-fluoro-, 5-fluoro-, and 4-methyl-5-fluoro-APTRA (Figure 1) were prepared and their properties as specific chelators studied.

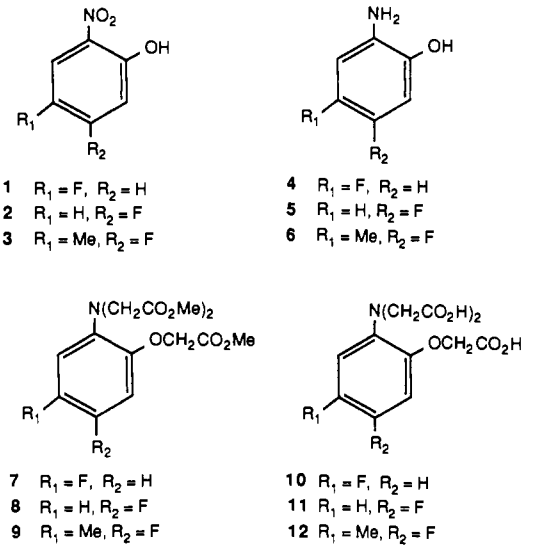

FIGURE 1: Structures of fluorinated APTRA derivatives.

Materials and Methods

Synthesis of Fluorinated Magnesium Selective Chelators. The synthesis of chelators **10**–**12** (see Figure 1) was accomplished by alkylation of the aminophenol derivatives **4**–**6** and subsequent hydrolysis of the resultant esters **7**–**9**. The aminophenols were obtained by catalytic hydrogenation of nitrophenols **1**–**3**. Fluorinated nitrophenols **1** and **2** are commercially available (Lancaster Synthesis, Windham, NH; Aldrich Chemical Co., Milwaukee, WI), and 4-methyl-5-fluoro-2-nitrophenol (**3**) was prepared by the route previously described (Levy et al., 1986). Conversion of the 4-methyl-5-fluoro chelator **12** to the acetoxymethyl ester appropriate for loading into cells was performed by Molecular Probes (Junction City, OR) via hydrolysis to the acid and reesterification with acetoxymethyl bromide. Thin-layer chromatography and column chromatography were carried out on silica gel. NMR spectra were obtained by using either a Nicolet NT360 or a GE GN500 NMR spectrometer. Melting points were obtained with a Fisher-Johns apparatus and are uncorrected. Elemental analyses were performed by Galbraith Laboratories (Knoxville, TN).

2-Amino-4-fluorophenol (**4**). Catalytic hydrogenation of 23.5 mmol of 2-nitro-4-fluorophenol in 75 mL of ethanol over 600 mg of 10% Pd/C was carried out at atmospheric pressure. After the uptake of hydrogen ceased, the catalyst was filtered off and the solvent evaporated to give a 95% yield of **4** as gray crystals. A sample recrystallized from benzene/hexane had mp 148–149 °C [lit. (Tikhonina et al., 1975) mp 135–136 °C].

2-Amino-5-fluorophenol (**5**). In a similar manner reduction of 2-nitro-5-fluorophenol gave **5** in 88% yield. A sample recrystallized from benzene/hexane had mp 141–143 °C.

2-Amino-4-methyl-5-fluorophenol (**6**). Catalytic reduction of nitro compound **3** produced **6** in 90% yield with a mp of 141–143 °C (benzene/hexane) [lit. (Frischkorn et al., 1982) mp 130–132 °C]: NMR (CD_3OH) 1.98 (d, J = 1.5 Hz, 3 H, $ArCH_3$), 6.32 (d, J = 10.6 Hz, 1 H, Ar H), 6.46 (d, J = 8.0 Hz, 1 H, Ar H).

2-Amino-4-fluorophenol-N,N,O-triacetic Acid Trimethyl Ester (**7**) (*4F-APTRA*). A mixture of 30 mmol of aminophenol **4**, 120 mmol of proton sponge [bis(1,8-dimethylamino)naphthalene], 120 mmol of methyl bromoacetate, and 6 g of sodium iodide in acetonitrile (45 mL) was refluxed under

[1] Abbreviations: APTRA, 2-aminophenol-*N*,*N*,*O*-triacetic acid; 4F-APTRA, 2-amino-4-fluorophenol-*N*,*N*,*O*-triacetic acid; 5F-APTRA, 2-amino-5-fluorophenol-*N*,*N*,*O*-triacetic acid; MF-APTRA, 2-amino-4-methyl-5-fluorophenol-*N*,*N*,*O*-triacetic acid; BAPTA, 1,2-bis(2-aminophenoxy)ethane-*N*,*N*,*N*′,*N*′-tetraacetic acid; 4F-BAPTA, 1,2-bis(2-amino-4-fluorophenoxy)ethane-*N*,*N*,*N*′,*N*′-tetraacetic acid; 5F-BAPTA, 1,2-bis(2-amino-5-fluorophenoxy)ethane-*N*,*N*,*N*′,*N*′-tetraacetic acid; MF-BAPTA, 1,2-bis(2-amino-4-methyl-5-fluorophenoxy)ethane-*N*,*N*,*N*′,*N*′-tetraacetic acid; EDTA, ethylenediamine-*N*,*N*,*N*′,*N*′-tetraacetic acid; EGTA, ethylene glycol bis(β-aminoethyl ether)-*N*,*N*,*N*′,*N*′-tetraacetic acid; Hepes, 4-(2-hydroxyethyl)-1-piperazineethanesulfonic acid; Tris, tris(hydroxymethyl)aminomethane.

argon for 60 h. The cool reaction mixture was filtered, diluted with ethyl acetate, and then filtered again from the additional precipitate. The crude reaction mixture was chromatographed on silica and the product eluted with 7:3 hexane/ethyl acetate in 58% yield. After recrystallization from benzene, the product had mp 78–79 °C: NMR ($CDCl_3$) 3.73 (s, 6 H, CO_2CH_3), 3.78 (s, 3 H, CO_2CH_3), 4.18 [s, 4 H, $N(CH_2CO_2Me)_2$], 4.61 [s, 2 H, OCH_2CO_2Me], 6.6 (m, 2 H, Ar H), 6.8 (m, 1 H, Ar H). Anal. Calcd for $C_{15}H_{18}FNO$: C, 52.5; H, 5.28; N, 4.08. Found: C, 52.6; H, 5.48; N, 3.98.

2-Amino-5-fluorophenol-N,N,O-triacetic Acid Trimethyl Ester (**8**). This compound was prepared as described above, starting from aminophenol **5**, in 22% yield. A sample recrystallized from benzene/hexane had mp 68–69 °C: NMR ($CDCl_3$) 3.71 (s, 6 H, CO_2CH_3), 3.80 (s, 3 H, CO_2CH_3), 4.17 (s, 4 H, $N(CH_2CO_2Me)$, 4.67 (s, 2 H, OCH_2CO_2Me), 6.54 (dd, J = 2.73 and 9.8 Hz, 1 H, Ar H), 6.64 (ddd, J = 2.8, 8.3, and 8.3 Hz, 1 H, Ar H), 6.95 (dd, J = 5.9 and 8.8 Hz, 1 H, Ar H). Anal. Calcd for $C_{15}H_{18}FNO$: C, 52.5; H, 5.28; N, 4.08. Found: C, 53.1; H, 5.3; N, 4.02.

2-Amino-4-methyl-5-fluorophenol-N,N,O-triacetic Acid Trimethyl Ester (**9**). This compound was prepared similarly from aminophenol **6** in 62% yield. A sample recrystallized from benzene/hexane had mp 83–84 °C: NMR ($CDCl_3$) 2.13 (d, J = 1.7 Hz, 3 H, Ar CH_3), 3.67 (s, 6 H, CO_2CH_3), 3.75 (s, 3 H, CO_2CH_3), 4.12 [s, 4 H, $N(CH_2COMe)_2$], 4.62 (s, 2 H, OCH_2CO_2Me), 6.49 (d, J = 10.4 Hz, 1 H, Ar H), 6.75 (d, J = 8.9 Hz, 1 H, Ar H). Anal. Calcd for $C_{16}H_2OFNO$: C, 53.7; H, 5.64; N, 3.92. Found: C, 54.4; H, 5.73; N, 3.81.

Hydrolysis of Substituted Aminophenol-N,N,O-triacetic Acid Trimethyl Esters. A solution of 2.0 g of ester in a mixture of 20 mL of 30% KOH and 20 mL of ethanol was stirred overnight at room temperature. The ethanol was evaporated and the solution acidified with 6 N HCl. The precipitated product was filtered, dried, and recrystallized from acetone/hexane to yield pure product.

4-Fluoro-2-aminophenol-N,N,O-triacetic Acid (**10**). This compound was obtained in 70% yield, mp 184–185 °C: NMR [$(CD_3)_2CO$] 4.25 [s, 4 H, $N(CH_2CO_2H)$], 4.72 (s, 2 H, OCH_2CO_2H), 6.65 (ddd, J = 3.0, 7.9, and 8.8 Hz, 1 H, Ar H), 6.73 (dd, J = 2.9 and 10.9 Hz, 1 H, Ar H), 6.97 (dd, J = 5.5 and 8.4 Hz, 1 H, Ar H). Anal. Calcd for $C_{12}H_{12}FNO_7$: C, 47.8; H, 4.02; N, 4.65. Found: C, 48.0; H, 4.13; N, 4.48.

5-Fluoro-2-aminophenol-N,N,O-triacetic Acid (**11**). This compound was obtained in 68% yield, mp 171–172 °C: NMR [$(CD_3)_2CO$)]: 4.09 [s, 4 H, $N(CH_2CO_2H)_2$], 4.78 (s, 2 H, OCH_2CO_2H), 6.62 (ddd, J = 3, 8.5, and 8.5 Hz, 1 H, Ar H), 6.74 (dd, J = 3 and 10.5 Hz), 7.07 (dd, J = 6 and 8.5 Hz, 1 H, Ar H). Anal. Calcd for $C_{12}H_{12}FNO_7$: C, 47.8; H, 4.02; N, 4.65. Found: C, 48.2; H, 4.00; N, 4.47.

5-Fluoro-4-methyl-2-aminophenol-N,N,O-triacetic Acid (**12**). This material was obtained in 71% yield as the hydrochloride, mp 238–240 °C dec: NMR (D_2O) 2.18 (d, J = 1.1 Hz, 3 H, Ar CH_3), 4.64 (s, 2 H, OCH_2CO_2H), 4.79 [s, 4 H, $NHCl(CH_2CO_2H)_2$], 6.77 (d, J = 10.9 Hz, 1 H, Ar H), 7.28 (d, J = 7.5 Hz, 1 H, Ar H). Anal. Calcd for $C_{12}H_{13}ClFNO_7$: C, 44.4; H, 4.29; N, 3.98. Found: C, 44.3; H, 3.81; N, 3.85.

K_D Determination. The K_D for all chelators was determined in a solution made up to resemble the intracellular milieu of mammalian cells. The solution contained 115 mM KCl, 20 mM NaCl, and 10 mM Hepes buffered with Tris base to pH 7.1. The K_D's were measured by following the decrease in absorbance at 248 nm, which occurred as magnesium or calcium was added to the solution containing 0.33 mM (0.25 mM for 4F-APTRA) chelator. Absorbances were measured at 25 and 37 °C by using a Hewlett-Packard diode array (Model 8451A) or a Gilford spectrophotometer (Model 240). K_D values were determined from two separate types of plot. A Lineweaver–Burk plot of $1/Mg_f$ vs $1/\Delta Abs$ gives $-1/K_D$ as the x intercept. Mg_f was calculated from the equation

$$Mg_f = Mg_t - \left(\frac{\Delta Abs}{\text{Abs no Mg} - \text{Abs with excess Mg}}[\text{total chelator}]\right)$$

where ΔAbs = Abs with no Mg − Abs at a given Mg. K_D's were also calculated from a Hill plot of log Mg_f vs log [ΔAbs/(Abs at a given Mg − Abs at excess Mg)]. In order to obtain K_D values in a short period of time corresponding to concentrations similar to those utilized in intracellular studies, UV measurements were used. There was some indication that at higher concentrations of chelator the stoichiometry may be more complex.

NMR Spectroscopy. Studies on solutions of these chelators were performed on a Nicolet NT-360 NMR spectrometer using a 5-mm ^1H probe tuned to 339.7 MHz for ^{19}F detection. The sample was shimmed on the H_2O resonance, and we routinely obtained a (nonspinning) line width at half-height of 0.01 ppm. For studies on chelator-loaded erythrocytes, we used a 20-mm fluorine probe (Doty Scientific) tuned to 339.7 MHz. In these studies we also shimmed on H_2O and routinely obtained a nonspinning line width at half height of <0.1 ppm. We used a 40° pulse angle, a 500-μs delay, and a 205-ms acquisition time. As a consequence of the similar spin–lattice relaxation rates of free and magnesium-complexed chelators, we have found that the ratio of the resonance intensities is unaltered under rapid-pulsing conditions (Levy et al., 1987; Murphy et al., 1986). In the present case, inversion recovery measurements of spin–lattice relaxation gave T_1 values of 1.34 ± 0.07 and 1.39 ± 0.03 s for the uncomplexed and magnesium-complexed 5F-APTRA. Shifts for the chelator were measured from the standard 6-fluorotryptophan. Areas under resonances were determined by cutting and weighing.

Erythrocyte Preparation. Blood was drawn into heparin-containing syringes. The plasma and buffy coat were discarded, and the cells were washed 3 times at 10000g in a sodium wash solution containing 145 mM NaCl and 5 mM Hepes adjusted to pH 7.4 with Tris base at 37 °C. The cells were then suspended at a hematocrit of 4% in a loading buffer containing 145 mM NaCl, 1.25 mM $CaCl_2$, 5.0 mM sodium pyruvate, and 10 mM Hepes adjusted to pH 7.4 with Tris base plus 50 μM acetoxymethyl ester of MF-APTRA. The solution was gassed with 100% O_2. After a 20-min incubation at 37 °C, the cells were centrifuged and resuspended in the loading buffer minus the acetoxymethyl ester of the chelator.

Results

UV Absorption Studies. The interaction of the fluorinated APTRA derivatives with Mg^{2+} and Ca^{2+} ions can be followed by UV absorption or ^{19}F NMR spectroscopy. The changes in the UV absorption spectra of 5F-APTRA that accompany magnesium complexation are illustrated in Figure 2A. In the absence of divalent cations, the spectrum has three maxima at 234, 248, and 291 nm. The spectrum is thus seen to be qualitatively similar to the BAPTA UV spectrum described by Tsien (1980), which exhibits absorption maxima at 254 and 287 nm. Magnesium complexation by 5F-APTRA causes a large decrease in absorbance of both the 248- and 291-nm peaks, with a considerably smaller reduction in the absorbance at 234 nm, and the dependence on Mg^{2+} concentration is suggestive of a dissociation constant in the millimolar range.

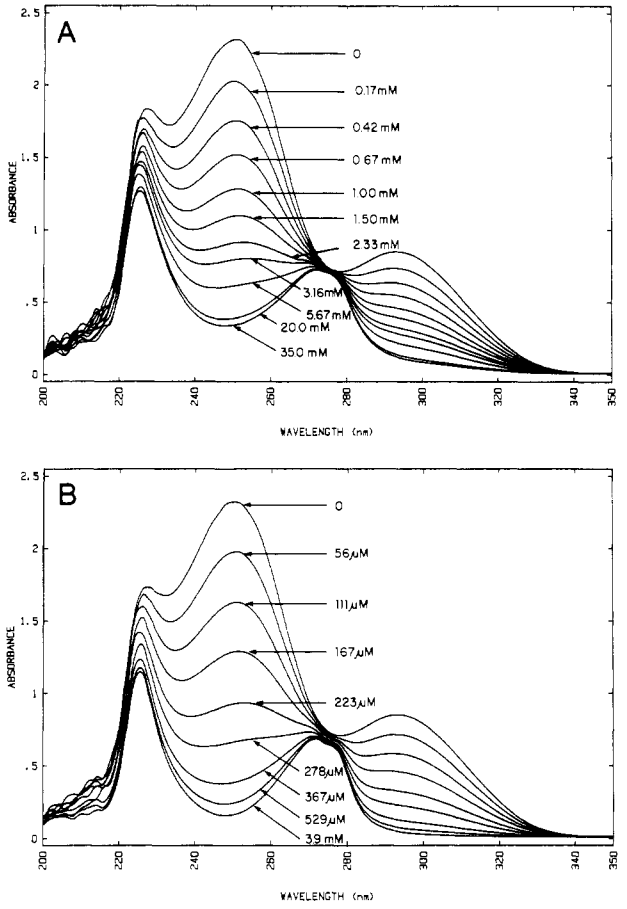

FIGURE 2: UV absorption spectrum of 5F-APTRA (0.33 mM) as a function of magnesium concentration (A) or calcium concentration (B). Spectra were obtained at 25 and 37 °C in 115 mM KCl, 20 mM NaCl, and 10 mM Hepes buffered with Tris base to pH 7.1.

Table I: Magnesium Equilibrium and Kinetic Rate Constants for Fluorinated APTRA Derivatives

chelator	K_D[a] (mM) 25 °C	37 °C	k_{-1}[b] (s^{-1})	k_1[b] (M^{-1} s^{-1})
MF-APTRA	1.0 ± 0.1	0.6 ± 0.1	7.63×10^2	7.48×10^5
5F-APTRA	1.8 ± 0.1	0.9 ± 0.1	9.80×10^2	5.38×10^5
4F-APTRA	4.8 ± 0.9	3.1 ± 0.2	1.88×10^3	3.88×10^5

[a] K_D values are means ± SEM. [b] Determined at 25 °C.

Analysis of the data using a Lineweaver–Burk or Hill plot (Dixon & Webb, 1979) showed the stoichiometry for Mg^{2+}–5F-APTRA chelation to be consistent with a 1:1 complex. The corresponding dissociation constants for magnesium for each of the APTRA derivatives determined in this way are summarized in Table I. The fluorine and methyl substituents change the Mg^{2+} dissociation constants in an analogous manner to the change that similar substitution produces for the Ca^{2+} affinities of fluorinated BAPTA derivatives (Smith et al., 1983; Levy et al., 1987). Both the spectral perturbations and the changes in Mg^{2+} dissociation constants are found to be consistent with a model for complexation involving the nitrogen atom, analogous to that postulated by Tsien for BAPTA and verified by direct crystallographic analysis of the Ca^{2+}–5F-BAPTA complex (Gerig et al., 1987).

The spectral perturbations resulting from the complexation of Ca^{2+} with 5F-APTRA are illustrated in Figure 2B. As is evident from a comparison of parts A and B of Figure 2, the mode of interaction of 5F-APTRA with the two divalent metal ions is similar. Ca^{2+} dissociation constants derived from these studies are summarized in Table II.

Table II: Calcium Equilibrium and Kinetic Rate Constants for Fluorinated APTRA Derivatives

chelator	K_D[a] (μM) 25 °C	37 °C	k_{-1}[b] (s^{-1})	k_1[b] (M^{-1} s^{-1})
MF-APTRA	12 ± 6	7 ± 4	5.55×10^3	4.63×10^8
5F-APTRA	38 ± 10	25 ± 10	9.09×10^3	2.39×10^8
4F-APTRA	167 ± 10	86 ± 3	1.32×10^4	7.93×10^7

[a] K_D values are means ± SEM. [b] Determined from ^{19}F NMR at 25 °C.

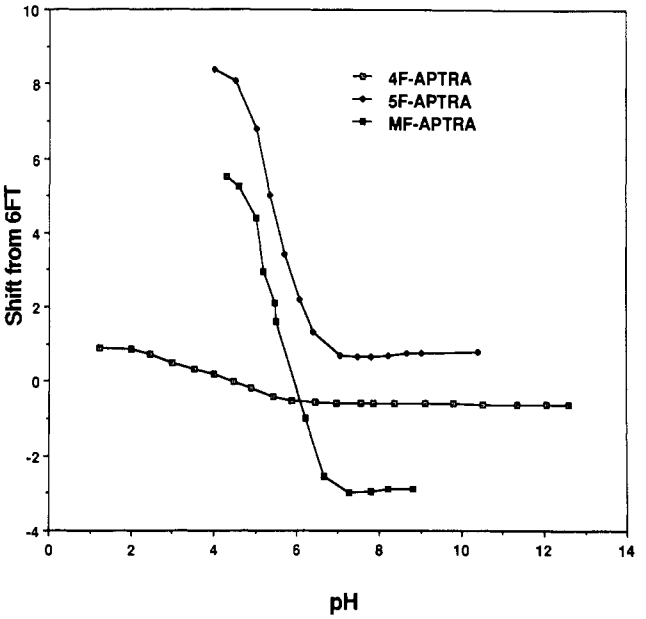

FIGURE 3: ^{19}F chemical shifts for 4F-APTRA, 5F-APTRA, and MF-APTRA as a function of pH. NMR spectra were obtained in the same buffer system described in Figure 2.

Fluorinated APTRA derivatives exhibit lower K_D values for calcium than for magnesium as is the case with EDTA, the chelator from which APTRA is conceptually derived. Ratios of $10^{1.9}$, $10^{1.6}$, and $10^{1.5}$ for K_D^{Mg}/K_D^{Ca} were obtained for MF-, 5F-, and 4F-APTRA, respectively. These compare with a ratio of $10^{1.8}$ reported for EDTA (Martin, 1984).

In conclusion, APTRA and BAPTA show similar changes of their UV absorption spectra induced by either Mg^{2+} or Ca^{2+} complexation, indicating a similar mode of complexation in which the hybridization of the amino group is altered from an aniline-like structure to a tetrahedral nitrogen that interacts directly with the metal ion.

^{19}F NMR Studies of pH Dependence. The pH dependence of the fluorine NMR resonance of the three APTRA derivatives shown in Figure 3 was determined in 115 mM KCl, 20 mM NaCl, and 10 mM Hepes–Tris. From these data, it is determined that the 4F, 5F, and MF derivatives exhibit pK values of 4.15, 5.45, and 5.50, respectively. Undoubtedly, the fluorine shift will be highly sensitive to protonation of the amino group, and relatively insensitive to titration of the carboxyl groups, so that the former is likely the protonation which is being monitored by the ^{19}F NMR. These low pK values are consistent with the results determined for the fluorinated BAPTA derivatives and show that these derivatives will be relatively insensitive to changes in pH in the physiologically interesting range.

^{19}F NMR Studies of Magnesium Complexation. A 1:1 stoichiometry for APTRA complexation with Mg is consistent with the UV absorbance data reported above. (However, since the APTRA derivatives contain only five potential metal ion ligands, additional ligation with other molecules, presumably

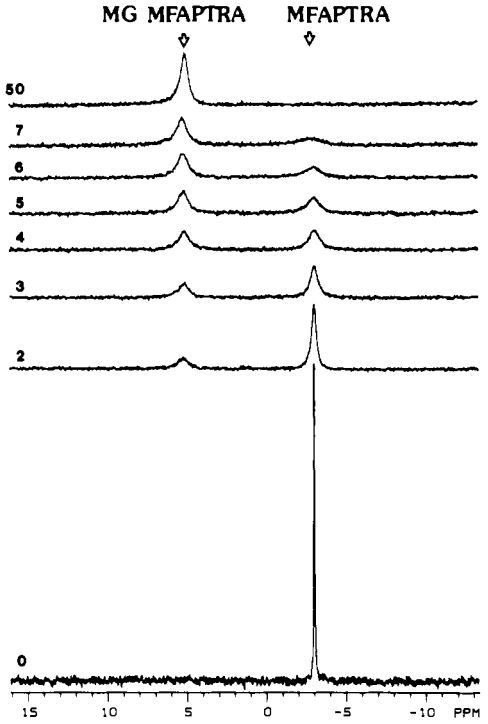

FIGURE 4: ^{19}F NMR spectra of MF-APTRA (5 mM) as a function of added (total) magnesium concentration. Spectra were obtained by using a ±5 kHz sweep width, 4K block size for a 205-ms acquisition time, and a 40° flip angle.

water, is probable.) Given this 1:1 stoichiometry, the exchange between free and complexed magnesium ions can be described by

$$Mg^{2+} + APTRA \underset{k_{-1}}{\overset{k_1}{\rightleftharpoons}} MgAPTRA \qquad (1)$$

A series of ^{19}F NMR spectra obtained for a solution containing 5 mM MF-APTRA as a function of added magnesium ion concentration is shown in Figure 4. As is apparent from these data, the magnesium ions are in slow exchange with the MF-APTRA. At equilibrium, the fractions of free and magnesium-complexed APTRA are related by

$$[APTRA]/\tau_F = [MgAPTRA]/\tau_B \qquad (2)$$

where τ_F and τ_B are the lifetimes of the free and magnesium-complexed chelator, respectively. By comparison with eq 1, it is seen that $\tau_B = (k_{-1})^{-1}$ and $\tau_F = (k_1[Mg])^{-1}$. Exchange contributions to the line widths of the ^{19}F resonances in the slow-exchange limit are given by $\nu_{1/2}^{bound} = k_{-1}/\pi$ and $\nu_{1/2}^{free} = [Mg]k_1/\pi$. These relationships are borne out by the data in Figure 4, and it is noted in particular that the observed ^{19}F line width for the MgMF-APTRA complex is constant, while the ^{19}F line width for the uncomplexed MF-APTRA depends in the expected way on the magnesium concentration. Similar ^{19}F spectra were obtained for 5F-APTRA as a function of magnesium concentration. The kinetic rate constants were extracted from the data by using a two-site exchange program supplied with the Nicolet data system and are included in Table I. By use of the dissociation rate constants (k_{-1}) determined from the NMR spectra and the equilibrium constants (K_D) derived above from UV absorbance data, the association rate constants (k_1) for the magnesium complexation with MF-APTRA and 5F-APTRA were calculated and are summarized in Table I. The association rate constants (k_1) so determined are roughly 3 orders of magnitude lower than the diffusion-controlled rates that have been determined for the association of calcium ions with similar chelators (Smith et al., 1983; Jackson et al., 1987).

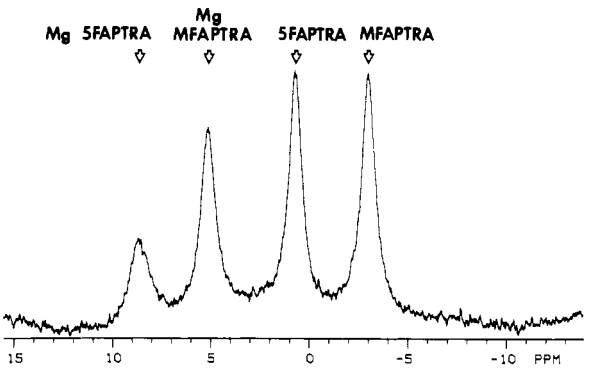

FIGURE 5: ^{19}F NMR spectrum of a solution containing 5 mM MF-APTRA, 5 mM, 5F-APTRA, and 6 mM total Mg^{2+} (added as $MgCl_2$). Spectral parameters were as in Figure 4.

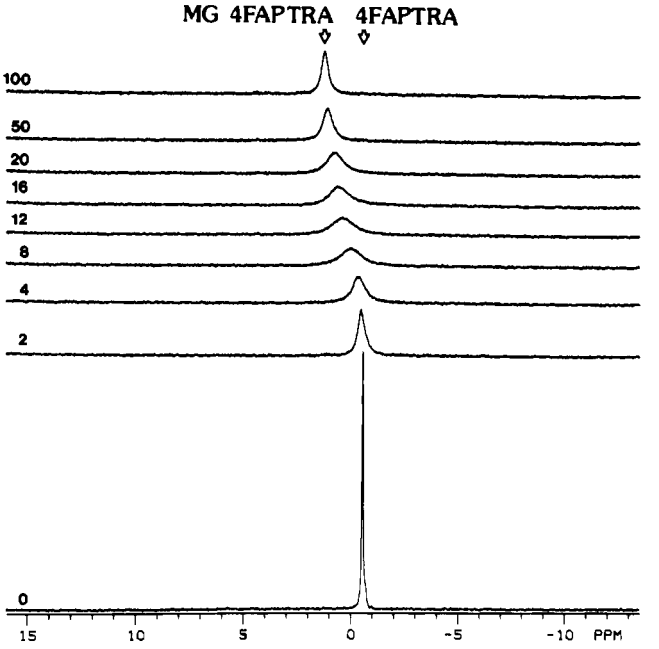

FIGURE 6: ^{19}F NMR spectra of 4F-APTRA (5 mM) as a function of added (total) magnesium ion concentration. Spectral parameters were as in Figure 4.

The slow exchange kinetics and chemical shift differences that characterize the magnesium complexes of 5F-APTRA and MF-APTRA allow us to compare the ratio of the magnesium dissociation constants by using an NMR measurement of a solution containing both indicators. The ^{19}F spectrum obtained on a solution containing 5 mM MF-APTRA, 5 mM 5F-APTRA, and 6 mM Mg^{2+} is shown in Figure 5. Since the free Mg^{2+} concentration is fixed and identical for both chelators, the dissociation constants are related by the intensity ratios

$$\frac{[\text{MF-APTRA}]}{[\text{MgMF-APTRA}]}\frac{1}{K_D{}^{MF}} = [Mg^{2+}]^{-1} = \frac{[\text{5F-APTRA}]}{[\text{Mg5F-APTRA}]}\frac{1}{K_D{}^{5F}}$$

A comparison of the intensity ratios for the MF- and 5F-APTRA derivatives yields a dissociation constant ratio of $K_D{}^{5F}/K_D{}^{MF} = 1.8$, in good agreement with the determination based on the UV absorption spectra.

In contrast to the slow exchange kinetics that characterize the association of Mg^{2+} ions with MF-APTRA and 5F-APTRA, the complexation of Mg^{2+} with 4F-APTRA falls into the fast to intermediate exchange limit when studied at 339.7

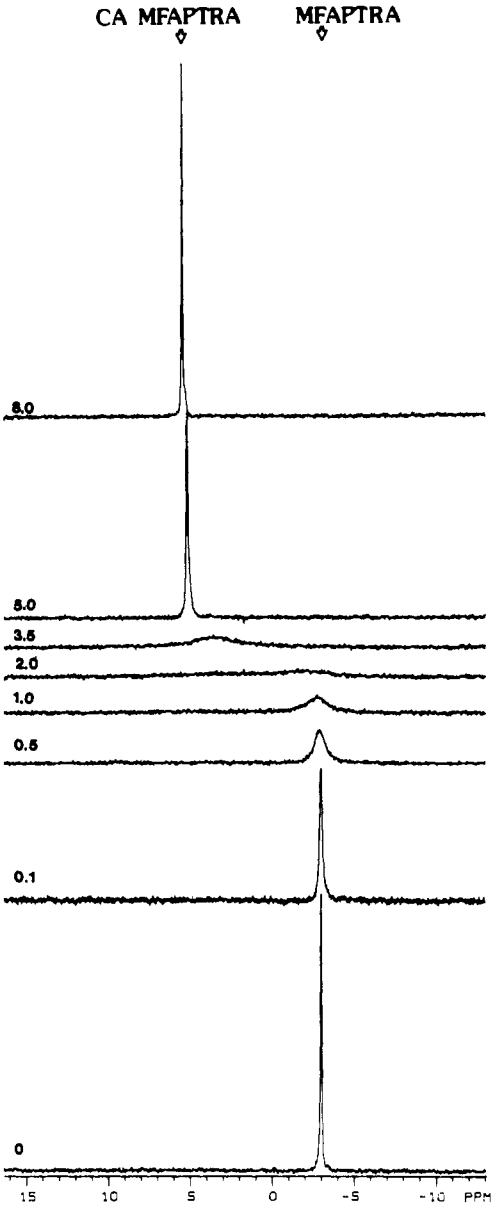

FIGURE 7: ^{19}F NMR spectra of 5 mM MF-APTRA as a function of added total Ca^{2+}. Spectral parameters were as in Figure 4.

MHz and 25 °C (Figure 6). Kinetic rate constants describing the exchange of Mg^{2+} ions with 4F-APTRA were extracted by analysis of spectra simulated for a two-site exchange model using a program supplied on the Nicolet NT-360 spectrometer. This kinetic behavior is seen to be closely analogous to the results obtained for calcium complexation with the corresponding series of fluorinated BAPTA derivatives. Thus, calcium is observed to be in slow exchange with 5F-BAPTA (Smith et al., 1983) and with 4-methyl-5-fluoro-BAPTA (Levy et al., 1987) but in fast to intermediate exchange with 4F-BAPTA (Smith et al., 1983).

^{19}F NMR Studies of Calcium Complexation. Although complexation of each of the fluorinated APTRA derivatives with Ca^{2+} ions was found to produce shifts similar to those obtained for Mg–APTRA complexes, the exchange kinetics in all cases were found to fall into the intermediate to fast range when studied at 339.7 MHz. Thus, even the chelator with the highest relative affinity for Ca^{2+}, MF-APTRA, yields an intermediate exchange pattern when analyzed at 339.7 MHz (Figure 7). Exchange data were similarly analyzed as in the case of the 4F-APTRA by using a two-site chemical exchange formalism, and the kinetic parameters thus determined are summarized in Table II. It is worth noting that attempts to use a fast-exchange approximation to describe the data for 5F-APTRA and MF-APTRA gave significant errors.

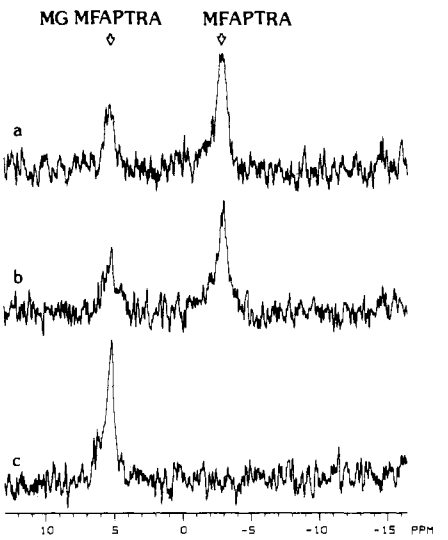

FIGURE 8: ^{19}F NMR spectra of MF-APTRA-loaded erythrocytes at 37 °C: (a) initial spectrum; 17-min accumulation; (b) second accumulation after addition of 6 mM $MgCl_2$ extracellular; (c) accumulation subsequent to the addition of the ionophore A23187. In spectrum c, the bound MF-APTRA resonance actually corresponds to a mixture of magnesium and calcium complexed chelator since calcium was present in the buffer. Other spectral parameters were ±5 kHz spectral width, 40° flip angle, pulse recycle time of 205 ms, and 5000 acquisitions.

Determination of Cytosolic Free Mg Concentration in Human Erythrocytes. In order to evaluate the use of the fluorinated APTRA derivatives for the determination of intracellular free magnesium ion levels, the acetoxymethyl derivative of MF-APTRA was prepared and loaded into erythrocytes as described under Materials and Methods. As in the case with the fluorescent and fluorinated calcium chelators, it was anticipated that cellular esterases would cleave the acetoxymethyl ester groups. This was indeed found to be the case, and the ^{19}F NMR spectra obtained for MF-APTRA acetoxymethyl ester loaded erythrocytes are shown in Figure 8. As in the in vitro studies, two resonances are observed corresponding to free and magnesium-complexed chelator. Previous determinations in these cells demonstrated that cytosolic free calcium is present at too low a level to significantly complex the indicator (Levy et al., 1987; Murphy et al., 1986). In addition, since in most cases the kinetics of calcium complexation is sufficiently rapid to lead to a single, broadened resonance, as long as the uncomplexed APTRA resonance remains unshifted and unbroadened we can be sure that Ca–APTRA complexation is not occurring. The cytosolic free magnesium concentration can be directly determined from the relation

$$[Mg^{2+}] = K_D[\text{MgMF-APTRA}]/[\text{MF-APTRA}]$$

and is found to be 0.25 mM for human erythrocytes. The addition of extracellular magnesium ions to a level of 6 mM had a negligible effect on the cytosolic free magnesium ion concentration, as shown in Figure 8b. Addition of the ionophore A23187 resulted in collapse of the magnesium gradient, thereby leading to essentially complete complexation of the intracellular indicator (Figure 8c).

Discussion

The determination of intracellular ionized free magnesium levels in cells is a problem of long standing to which a number of methods have been applied. As discussed in the introduc-

tion, each of these approaches is subject to significant limitations.

The present results demonstrate that chelator structures related to *o*-aminophenol-*N*,*N*,*O*-triacetate (APTRA) exhibit suitable K_D's for magnesium, protons, and calcium ions to function as reasonable indicators for magnesium under typical physiological conditions. The 1:1 stoichiometry of magnesium chelation determined from the UV absorbance data is consistent with expectations based on structurally analogous EDTA complexes (Stezowski et al., 1973). The three fluorinated APTRA derivatives studied display a range of magnesium K_D values that allow accurate measurements to be made over a range of cytosolic Mg^{2+} values. The MF-APTRA and 5F-APTRA derivatives appear to be most useful for such applications since Mg_i can be readily calculated from a ratio of the areas determined for the resonances corresponding to the uncomplexed and magnesium-complexed species. In contrast, since 4F-APTRA is in fast exchange, it requires the introduction of a suitable internal standard from which the ^{19}F chemical shift of the indicator can be determined. There is also some evidence of intermediate exchange at 339.7 MHz for 4F-APTRA at 25 °C. In general, the optimal selection of the fluorinated indicators will depend on the magnetic field strength and temperature, and predictions of exchange behavior as a function of magnetic field strength can be made by using the data supplied in Tables I and II.

Although the Ca^{2+} dissociation constants determined for each of the APTRA derivatives are significantly lower than those for Mg^{2+}, they are still considerably higher than the typical cytosolic ionized calcium levels. Nevertheless, it is reasonable to evaluate the possibility that calcium chelation could interfere with the determination of cytosolic magnesium levels under conditions of elevated cytosolic calcium. The distinction between the response of the fluorinated APTRA derivatives to Ca^{2+} and Mg^{2+} is based both on the K_D values and on differences in the kinetics of chelation. Thus, in most cases, calcium exchange results in a single, shifted broadened resonance, while for MF- and 5F-APTRA magnesium chelation will lead to the observation of separate resonances corresponding to complexed and free chelator. Therefore, as long as there is no broadening or shift in the uncomplexed APTRA resonance we can be sure that Ca–APTRA chelation is not a problem.

The cytosolic free magnesium level of 0.25 mM obtained for human erythrocytes in this study agrees well with previous measurements of 0.2–0.4 mM (Gupta et al., 1978; Flatman & Lew, 1977). The lack of change in cytosolic free magnesium upon raising the extracellular magnesium to 6 mM is consistent with the data of others [see Grubbs and Maguire (1987) and references cited therein] suggesting that intracellular magnesium is slow to exchange or equilibrate with extracellular magnesium. However, we can measure an increase in cytosolic free magnesium that occurs upon addition of the divalent cation ionophore A23187.

One of the more surprising results of the present studies is the observation that the expected relationship between the dissociation constants for calcium and magnesium, viz., $K_D^{Mg}/K_D^{Ca} \gg 1$, is not reflected in the dissociation rate constants for which $k_{-1}^{Mg}/k_{-1}^{Ca} < 1$. Thus, although for a given free ion concentration the calcium will be more fully complexed than the magnesium, the calcium complexes are less stable, resulting in more rapid exchange kinetics. This apparent anomaly reflects the dramatic differences between the association rate constants for Ca^{2+} and Mg^{2+}, with the former exceeding the latter by 3 orders of magnitude. Since the association rate constants obtained for Ca^{2+} are close to the diffusion limit (Smith et al., 1983; Jackson et al., 1987), this result implies that only 1 in 1000 collisions of Mg^{2+} with the APTRA chelators will result in the formation of a complex. The likely interpretation of this result would appear to be the tighter association of the hydrated water molecules to the magnesium ion, since these water molecules must be displaced for the complex to form. As discussed by Diebler et al. (1969) for alkaline earth ions, the ligand substitution rates for Ca^{2+} are always at least 3 orders of magnitude greater than for Mg^{2+}, irrespective of the ligand. This conclusion is qualitatively consistent with the fact that Mg^{2+} also forms a longer lived complex with the chelators as reflected in the relative k_{-1} values.

Several other aspects of the use of fluorinated APTRA derivatives for the determination of cytosolic magnesium levels merit comment. First, the association rate constants for magnesium ions determined for these derivatives are roughly 3 orders of magnitude above the value of 5.55×10^2 M^{-1} s^{-1} that has been reported for the indicator Eriochrome blue SE (Scarpa & Brinley, 1981). This difference implies a comparably better intrinsic time resolution achievable by the indicator, although, in fact, the time resolution achievable in ^{19}F NMR studies will be determined by sensitivity considerations. Second, the concentration of APTRA-complexed magnesium ions typical in these studies will be similar in magnitude to the concentration of free magnesium ions in the cell. This implies that the problem of buffering of magnesium transients resulting from the introduction of the indicator will be less severe than for the analogous measurements of cytosolic calcium ions in which calcium-complexed indicator concentrations are generally much greater than the free calcium ion levels being measured. Finally, it is noted that the combination of the APTRA structure and its associated ionic specificities with the fluorophores developed by Tsien and co-workers (Grynkiewicz et al., 1985) is straightforward, and evaluations of fluorescent cellular magnesium indicators prepared in this way are in progress.

ACKNOWLEDGMENTS

We greatly appreciate the excellent technical assistance of Scott Gabel, as well as useful input from Drs. Michael E. Perlman and Donald G. Davis. We thank Robin Sorrell for secretarial assistance.

Registry No. **1**, 394-33-2; **2**, 446-36-6; **3**, 83341-28-0; **4**, 399-97-3; **5**, 53981-24-1; **6**, 83341-37-1; **7**, 114199-91-6; **8**, 114199-92-7; **9**, 114199-93-8; **10**, 114199-94-9; **10** Ca complex, 114220-99-4; **10** Mg complex, 114199-97-2; **11**, 114199-95-0; **11** Ca complex, 114200-00-9; **11** Mg complex, 114199-98-3; **12**, 114199-96-1; **12** Ca complex, 114200-01-0; **12** Mg complex, 114199-99-4; Ca, 7440-70-2; Mg, 7439-95-4.

REFERENCES

Altura, B. M., & Altura, B. T. (1981) *Fed. Proc., Fed. Am. Soc. Exp. Biol. 40*, 2672–2679.

Bond, M., Vadasz, G., Somlyo, A. V., & Somlyo, A. P. (1987) in *Cell Calcium Metabolism 1987, Proceedings of the Seventh International Washington Spring Symposium* (Fiskum, G., Ed.) Academic, New York.

Brinley, F. J., & Scarpa, A. (1975) *FEBS Lett. 50*, 82–85.

Cohen, S. M. (1983) *J. Biol. Chem. 258*, 14294–14308.

Corkey, B. E., Duszynski, J., Rich, T. L., Matschinsky, B., & Williamson, J. R. (1986) *J. Biol. Chem. 261*, 2567–2574.

Diebler, H., Eigen, M., Ilgenfritz, G., Maass, G., & Winkler, R. (1969) *Pure Appl. Chem. 20*, 93–115.

Dixon, M., & Webb, E. C. (1979) in *Enzymes*, Academic, New York.

Flatman, P. W. (1984) *J. Membr. Biol. 80*, 1–14.
Flatman, P. W., & Lew, V. L. (1977) *Nature (London) 267*, 360–362.
Frischkorn, H., Pintschovius, V., & Schinzel, E. (1982) *Liebigs Ann. Chem.*, 1423–1433.
Fry, C. H. (1986) *Magnesium 5*, 306–316.
Fuji, S., Takemura, T., Wada, M., Akai, T., & Okuda, K. (1982) *Horm. Metab. Res. 14*, 161–162.
Garfinkel, L., & Garfinkel, D. (1984) *Biochemistry 23*, 3547–3552.
Gerig, J. T., Singh, P., Levy, L. A., & London, R. E. (1987) *J. Inorg. Biochem. 31*, 113–121.
Grubbs, R. D., & Maguire, M. E. (1987) *Magnesium 6*, 113–127.
Grynkiewicz, G., Poenie, M., & Tsien, R. Y. (1985) *J. Biol. Chem. 260*, 3440–3450.
Gupta, R. K., & Yushok, W. D. (1980) *Proc. Natl. Acad. Sci. U.S.A. 77*, 2487–2491.
Gupta, R. K., Benovic, J. L., & Rose, Z. B. (1978) *J. Biol. Chem. 253*, 6472–6476.
Henquin, J. C., Tamagawa, T., Nenquin, M., & Cogneau, M. (1983) *Nature (London) 301*, 73–74.
Iseri, L. T., & French, J. H. (1984) *Am. Heart J. 108*, 188–193.
Jackson, A. P., Timmerman, M. P., Bagshaw, C. R., & Ashley, C. C. (1987) *FEBS Lett. 216*, 35–39.
Levy, L. A., Murphy, E., & London, R. E. (1987) *Am. J. Physiol. 252*, C441–C449.
Lopez, J. R., Alamo, L., Caputo, C., Vergara, J., & Di Polo, R. (1984) *Biochim. Biophys. Acta 804*, 1–7.
Maguire, M. E., & Eros, J. J. (1980) *J. Biol. Chem. 255*, 1030–1035.
Martin, R. B. (1984) *Met. Ions Biol. Syst. 17*, 1–49.
Meissner, G., & Henderson, J. S. (1987) *J. Biol. Chem. 262*, 3065–3073.
Morris, P. G., Smith, G. A., Metcalfe, J. C., & Rodrigo, G. C. (1987) *Work in Progress 31*, presented at the Sixth Annual Meeting of the Society of Magnetic Resonance in Medicine, August 17, New York.
Murphy, E., Levy, L., Berkowitz, L. R., Orringer, E. P., Gabel, S. A., & London, R. E. (1986) *Am. J. Physiol. 251*, C496–C504.
Murphy, R. A., Bohr, D. F., & Newman, D. L. (1969) *Am. J. Physiol. 217*, 666–673.
Ostwald, T. J., & MacLennan, D. H. (1974) *J. Biol. Chem. 249*, 5867–5871.
Phillips, R. C., George, P., & Rutman, R. J. (1966) *J. Am. Chem. Soc. 88*, 2631–2640.
Rink, T. J., Tsien, R. Y., & Pozzan, T. (1982) *J. Cell Biol. 95*, 189–196.
Scarpa, A., & Brinley, F. J. (1981) *Fed. Proc., Fed. Am. Soc. Exp. Biol. 40*, 2646–2652.
Skou, J. (1975) *Q. Rev. Biophys. 7*, 401–434.
Smith, G. A., Hesketh, R. T., Metcalfe, J. C., Feeney, J., & Morris, P. G. (1983) *Proc. Natl. Acad. Sci. U.S.A. 80*, 7178–7182.
Stern, J. H., Knutsson, H. & MacLeish, P. R. (1987) *Science (Washington, D.C.) 236*, 1674–1678.
Stezowski, J. J., Countryman, R., & Hoard, J. L. (1973) *Inorg. Chem. 12*, 1749–1754.
Tikhonina, N. A., Timofeeva, G. I., Matrosov, E. J., Gilyarov, V. A., & Kabachnik, M. I. (1975) *Zh. Obshch. Khim. 45*, 2414–2422.
Tsien, R. Y. (1980) *Biochemistry 19*, 2396–2404.
Turlapaty, P. D. M. V., & Altura, B. M. (1980) *Science (Washington, D.C.) 208*, 198–200.
Veloso, D., Gwynn, R. W., Oskarsson, M., & Veech, R. L. (1973) *J. Biol. Chem. 248*, 4811–4819.
Wacker, W. E. C. (1987) *Magnesium 6*, 61–64.
Whang, R. (1987) *Magnesium 6*, 1–4.